*Journal of Intelligent and Robotic Systems* **24:** 295–311, 1999.



# $Q^2$ Symbolic Reasoning about Noisy Dynamic Systems

STEPHEN P. LINDER and ZBIGNIEW KORONA
*Mechanical, Industrial and Manufacturing Engineering, 'Northeastern University, Boston, MA 02115, USA; e-mail: zbigniew@coe.neu.edu*

MIECZYSLAW M. KOKAR
*Electrical and Computer Engineering, Northeastern University, Boston, MA 02115, USA; e-mail: kokar@coe.neu.edu*

(Received: 5 August 1998; accepted: 30 August 1998)

**Abstract.** Symbolic reasoning about continuous dynamic systems requires consistent qualitative abstraction functions and a consistent symbolic model. Classically, symbolic reasoning systems have utilized a *box* partition of the system space to achieve qualitative abstraction, but boxes can not provide a consistent abstraction. Our $Q^2$ methodology abstracts a provably consistent symbolic representation of noise-free general dynamic systems. However, the $Q^2$ symbolic representation has not been previously evaluated for efficacy in the presence of noise. We evaluate the effects of noise on $Q^2$ symbolic reasoning in the domain of maneuver detection. We demonstrate how the $Q^2$ methodology derives a symbolic abstraction of a general dynamic system model used in evaluating maneuver detectors. Simulation results represented by ROC curves show that the $Q^2$ based maneuver detector is superior to a box-based detector. While no method is consistent in the presence of noise, the $Q^2$ methodology is superior to the classic box's approach for deriving qualitative decisions about noisy dynamic systems.

**Key words:** qualitative abstraction, consistency, hybrid system, maneuver detection.

## 1. Introduction

Symbolic reasoning about a quantitative continuous plant requires a qualitative model of the plant with which to reason. Symbolic reasoning is preferred for many tasks because (Albus [1]):

- people relate better to reasoning based on alphanumeric symbols, planning can be performed more easily,
- symbolic reasoning can be used to achieve goals expressed in high-level symbolic language, and
- certain complex problems become computationally tractable when converted to symbolic representation.

Symbolic reasoning about continuous dynamic systems requires a *consistent symbolic model*, i.e., such a model in which any symbolic derivation holds in the underlying continuous dynamic system. More specifically, a consistent symbolic model for a dynamic system must derive correct conclusions regarding transitions among symbolic states given specific symbolic inputs.

When a qualitative model is created of a continuous plant we abstract *perceptual chunks* of information (Albus [1]). Multiple points in the continuous domain are condensed into perceptual chunks that represent single symbolic concepts. However, an arbitrary mapping from the continuous quantitative plant to a symbolic qualitative model may create a model that looses many important details about the plant. Indeed, so many details may be lost that the model can not support consistent reasoning about the plant. The qualitative reasoning community therefore has focused on developing chunks that promote consistent reasoning. Consistency must be preserved to have confidence in the symbolic reasoning perform (Genesereth and Nilsson [8]). The problem of symbolic reasoning about dynamic systems is also addressed by *hybrid control systems* (cf. Nerode and Kohn [18], Alur et al. [2], Branicky et al. [7]), although in that approach the model of a dynamic system is not fully symbolic, but, as the name suggests, it is a combination of both symbolic and quantitative representations.

The continuous model of a dynamic system has traditionally been partitioned with orthogonal, hyperplanes (Guckenheimer and Johnson [9]) to form *hyperboxes* (Kuipers [14, 15]). However, hyperboxes, with their orthogonal boundaries, do not take into account the interactions between plant variables produced by the dynamics of the plant and therefore do not produce consistent finite qualitative abstraction of the underlying continuous system (Strauss [20]). Hyperbox based hybrid systems can be forced to behave consistently by using smaller hyperboxes in areas of the system space that contain complex behavior (Kuipers [15]). This idea is similar to the methodology of finite-element analysis. Also, some authors have attempted to circumvent the inconsistencies in the hyperbox models by focusing on improving *switching* strategies between hyperboxes (Guckenheimer and Johnson [19]). In effect new chunks can be created by dithering between existing partitions*.

Kokar in his earlier papers on dimensional analysis (Kokar [10]) suggested that consistent abstractions could be better obtained by utilizing hyper-surfaces derived from the physical model of the plant. This work resulted in the $Q^2$ methodology for constructing consistent symbolic models of continuous noise-free dynamic plants (Kokar [11, 12]). $Q^2$ focuses on how to partition a system's space into a finite number of qualitative chunks that preserve consistency. $Q^2$'s partitions allow the construction of a symbolic representation of the underlying plant that is provably consistent for noise-free general dynamic systems. Also, the $Q^2$ approach creates

* This stress on switching strategies comes from work with non-linear systems. Non-linear plants are often modeled as a set of linear models, each model for a different operating point in the plant's domain, and a strategy for switching between models.

chunks that support a consistent qualitative model with simple switching strategies so we can use a finite state automaton as the qualitative (symbolic) representation of the plant.

Since we model a dynamic system with both quantitative and symbolic representations, we call our model a hybrid system. There is, however, a difference between the hybrid system approach as in (cf. Nerode and Kohn [18], Branicky et al. [7]), where the dynamic system is modeled by a hybrid automaton (Alur et al. [2]), and ours. While we also partition the state space by hypersurfaces (in the former approach they are called *exception sets*), we also have *qualitative events*, which are subsets of the Cartesian product of previous state, control input and elapsed time. As a result, we construct a finite state automaton (not a hybrid automaton), which can be used for purely symbolic reasoning. In the hybrid automaton, on the other hand, such events are generated by a dynamic process; in order to reason about such events one needs to solve the underlying differential equations as part of any reasoning with the automaton.

This paper gives a brief overview of the $Q^2$ theory and methodology (Kokar [12]) for constructing hybrid systems and shows through computer simulation that the $Q^2$ methodology is extensible to plants with noisy measurements. While measurement noise makes the hybrid system inconsistent, in the logical sense, noise is a fact of life. Successful $Q^2$ partitioning for a noise free system does not imply that it will also produce optimal reasoning for a noisy system. We must show that the $Q^2$ methodology not only produces consistent reasoning about noise-free plants but also produces reasoning that is superior to reasoning based on hyperboxes for noisy plants. The main goal of this paper is to show the superiority of the $Q^2$ approach to the box-partitioning approach under the existence of measurement noise. The superiority will be demonstrated for the task of aircraft maneuver detection. We show through simulations that:

- for reasonable levels of noise the $Q^2$ approach results in better maneuver detectors than the hyperbox approach,
- for high levels of noise both approaches perform equally poorly, and
- for noise free measurements the $Q^2$ approach results in no detection errors.

Although in this paper we are dealing with the issue of box vs. non-box partitioning in the context of the $Q^2$ methodology, the same problem arises in the hybrid automaton approach. While the hybrid automaton approach also allows for non-box partitions, in many cases the box partition is used. The reason for using box partitions is the complexity of computing non-box partitions (cf. Puri and Varaiya [19]). While the complexity of computation is a serious constraint on the applicability of the non-box partitions, in many cases, the partitions can be computed efficiently and the computation can be done off-line. For this reason, in this paper we focus on the advantages of the non-box partitioning.

## 2. Qualitative–Quantitative ($Q^2$) Abstraction

A typical approach to translating quantitative variables into qualitative symbols is to partition the quantitative state variables with some *critical values* of the quantitative variables. When the value of the quantitative state variable crosses a critical value, a *qualitative event* takes place (Antsaklis et al. [3], Lemmon et al. [16]). These events can be monitored and then used as input to a finite state automaton, which provides a qualitative model of the continuous plant. The automaton switches to a new state and generates control input associated with this state.

In the hyperbox representation, a qualitative event is triggered by a transition between boxes, with each event causing a corresponding transition between states in the automaton. A hyperbox representation constrains the critical values of one state variable independently of the values of the other state variables. In contrast to the hyperbox approach, the $Q^2$ approach allows the critical values for a quantitative variable to be functions of the other quantitative variables, which results in chunks that in general have more complex shapes than hyperboxes. The following section develops the $Q^2$ methodology for a plant modeled as a general dynamic system.

### 2.1. $Q^2$ APPLIED TO GENERAL DYNAMIC SYSTEMS

Our quantitative plant is modeled by a *General Dynamic System* (GDS). We use a set of *qualitative abstraction functions* to introduce a qualitative interpretation of the GDS model. The interpretation maps the continuous GDS model to a discrete finite state automaton. The qualitative abstraction functions and the automaton are combined to form a *Qualitative Dynamic System* (QDS) model of the qualitative plant.

A general dynamic system (Mesarovic and Takahara [17]) $S$ is an 8-tuple

$$S = (T, X, W, Q, P, f, g, \leqslant), \tag{1}$$

where:

- $T$ the time set with an order relation $\leqslant$ on it,
- $X$ the input set,
- $W$ the output set,
- $Q$ the inner state set,
- $P$ the input processes, functions $p\colon T \to X$,
- $f\colon$ $T \times Q \times p \to Q$, the state transition function,
- $g\colon$ $Q \to W$, the output function, and
- $\leqslant$ the order relation.

The $Q^2$ theory defines a qualitative dynamic system as a pair $(\Sigma, \chi)$. $\Sigma$ is a Deterministic Finite Automaton (DFA) represented as a 5-tuple

$$\Sigma = (\Lambda, \Omega, \Theta, \phi, \gamma) \tag{2}$$

with

$\Lambda$ a finite set of qualitative input events,

$\Omega$ a finite set of qualitative outputs,

$\Theta$ a finite set of qualitative states,

$\phi$: $\Lambda \times \Theta \rightarrow \Theta$, a qualitative state transition function, and

$\gamma$: $\Theta \rightarrow \Omega$, a qualitative output function.

$\chi$ is a set of three qualitative abstraction functions between the quantitative GDS and the qualitative QDS:

$\chi_p$: $T \times Q \times X \rightarrow \Lambda$, a qualitative input event abstraction function,

$\chi_Q$: $Q \rightarrow \Theta$, a qualitative state abstraction function, and

$\chi_W$: $W \rightarrow \Omega$, a qualitative output abstraction function.

Figure 1 shows graphically how the qualitative abstraction functions relate the parts of the GDS model to the QDS model. $\chi_Q$ maps quantitative states to qualitative states and $\chi_W$ maps quantitative outputs to qualitative outputs, but $\chi_p$ does not map quantitative inputs directly to qualitative inputs. $Q^2$ differs from other methods of qualitative abstractions by making qualitative inputs a function of not only quantitative inputs but also of quantitative states and time. This qualitative abstraction of $T \times Q \times X$ allows the QDS to be provably consistent abstraction of the GDS plant.

$Q^2$ postulates that for the QDS abstraction to be consistent any path taken in the schematic shown in Figure 1 has to result in the same abstraction. The qualitative output $\omega \in \Omega$ can be obtained from the quantitative state $q \in Q$ by either first deriving the quantitative output with the output function $g$ and then abstracting the qualitative output $\omega$ from continuous output $w \in W$ or by first abstracting the qualitative state $\theta \in \Theta$ and then using the qualitative output function to generate the

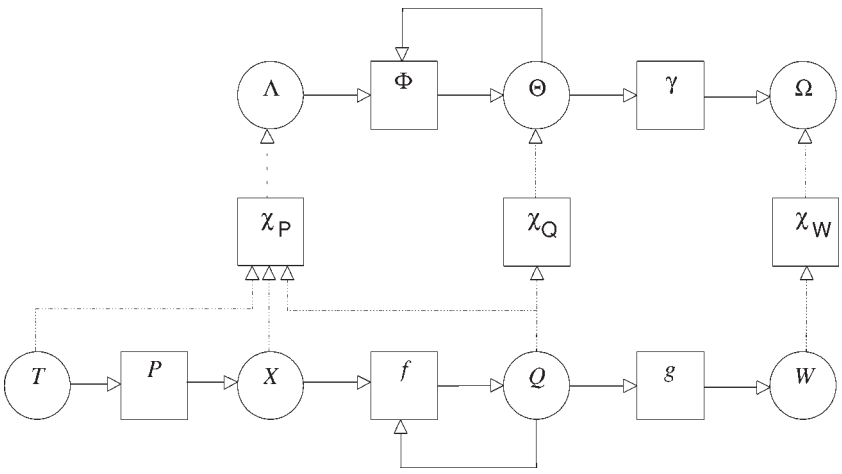


*Figure 1.* $Q^2$ abstraction of a General Dynamic System (GDS) using the qualitative abstraction functions $\chi_p$, $\chi_Q$ and $\chi_W$ to a Qualitative Dynamic System (QDS).

qualitative output $\omega$. Consistency is preserved if both paths are equivalent. Stated as a formal postulate we have

$$\gamma\big(\chi_Q(q)\big) = \chi_W\big(g(q)\big). \tag{3}$$

Similarly, the next qualitative state can be obtained from the current state $q$, input $x \in X$, and time $t \in T$ by either first deriving the next continuous state $q$ with the state transition function $f$ and then abstracting the qualitative state $\theta$, or by first abstracting the qualitative input event $\lambda \in \Lambda$ from $x$, $g$ and $t$, and then generating the next qualitative state $\theta$ with the qualitative state transition function $\phi$. Formally, we postulate

$$\phi\big(\Theta_0, \chi_p(t, q_0, x)\big) = \chi_Q\big(f(t, q_0, x)\big). \tag{4}$$

These two formal consistency postulates relate the abstraction of the inputs, state and output. The output of a GDS plant can not be partitioned without affecting the partition of the state; state can not be partitioned without affecting the partition of the input and output processes. After defining a partition of the output space of the GDS model, $Q^2$ uniquely determines the partitions of state and input, resulting in a consistent QDS representation.

Each distinguishing point in the output space translates into a *critical hypersurface* in the state space and correspondingly the hypersurface that partitions the state space translates into a critical hypersurface that partitions the $T \times X \times Q$ space. In the boxes approach we refer to these hypersurfaces as *hyperboxes* and in the $Q^2$ methodology we refer to these hypersurfaces as *hyperlimits*. Kuipers [14, 15] gives several examples of how hyperbox partitions are generated by dividing the output of a plant into intervals with a set of distinguishing points while Kokar [11, 12] gives examples of how distinguishing points generate $Q^2$ hyperlimits.

## 3. $Q^2$ and Maneuver Detection

In this section we show how the $Q^2$ methodology can be applied to maneuver detection. We define maneuver, describe the dynamics of a typical aerospace target, and then use $Q^2$ to develop a maneuver detector for a noise-free measurement. Next, we show how to extend our $Q^2$ models to accept noisy measurements.

### 3.1. OVERVIEW OF MANEUVER DETECTION

Since prompt detection of maneuvers can increase tracking accuracy the problem of maneuver detection has received great attention in the tracking literature (Bolger [6]). Most tracking algorithms use a Kalman filter, which requires an accurate model of the target's dynamics to estimate target position (Bar-Shalom and Fortmann [4]). A maneuver in tracking is an event that causes a mismatch between the model and target dynamics, resulting in increasing error in the position estimates.

If a maneuver is promptly detected and the model is switched accordingly the accuracy of the tracker increases greatly.

A typical radar tracker tracks an aircraft using a parsimonious* constant-velocity model and switches to a constant-acceleration model only after detecting an acceleration maneuver. The tracker cannot measure acceleration directly when detecting a maneuver because the constant-velocity model used by the Kalman filter does not include an acceleration term. A typical tracker must instead infer that acceleration has occurred when the predicted position estimates calculated by the Kalman filter begin to diverge from the position measurements. This difference, the *measurement residual* $\nu$ increases rapidly as the maneuver progresses because of the model mismatch.

The following section describes the plant used in our simulation, while Section 3.3 describes how to derive the $Q^2$ hyperlimits and hyperboxes for the plant used in maneuver detection.

### 3.2. PLANT DESCRIPTION

The plant we are tracking is described by a model (GDS) that is commonly used in evaluating the efficacy of Aircraft Tracking Systems (ATS) (Bar-Shalom and Fortmann [4], Korona and Kokar [13]). We have restricted our simulation to a one-dimensional model to reduce the complexity of the simulation. The state and output equations are

$$\begin{aligned} x(k+1) &= \mathbf{A}x(k) + \mathbf{B}u(k), \\ y(k) &= \mathbf{C}x(k) + \mathbf{D}u(k) + n(k), \end{aligned} \tag{5}$$

where

$$\mathbf{A} = \begin{vmatrix} 1 & T \\ 0 & 1 \end{vmatrix}, \qquad \mathbf{B} = \begin{vmatrix} T^2/2 \\ T \end{vmatrix}, \qquad \mathbf{C} = |1 \quad 0|, \quad \text{and} \quad \mathbf{D} = |0|. \tag{6}$$

$T$ is the time interval, $u(t)$ is the deterministic input and $n(t)$ is a Gaussian white noise process. There are several observations to make about the plant:

1. We utilize only position and not velocity measurements because most radar systems utilized in aviation collect only position measurements.
2. Deterministic acceleration input is considered constant during all sample intervals since the simulation's sampling period is much shorter than the duration of a plane maneuver (Bar-Shalom and Fortmann [4]).

The maneuver detectors we develop in the next section will measure the output of this plant at varying sample intervals, $\Delta t$; this scenario is typical for aviation

* Selecting the lowest order model is consistent with the variable state dimension approach to tracking; it is best to track a target using the lowest possible state dimension. If the order of the filter model is increased beyond the order of the data, an increase in the variance of the estimates results. See Bar-Shalom and Fortmann [4] for detailed discussion of this issue.

tracking systems that utilize several radars with different sampling rates (Blackman [5]).

### 3.3. QDS FOR MANEUVER DETECTION

The QDS model of the target utilized by the maneuver detector is derived for a GDS model of the target plant described in the previous section. Given a GDS model of the target with acceleration as output we can fully specify the qualitative abstraction functions and automaton used by our maneuver detector. The QDS automaton is then used to perform the symbolic reasoning needed to detect maneuvers. The resulting $Q^2$ maneuver detector derived in this section of the paper is for noise-free measurements of position $x$ and velocity $v$ that reflect accurately the state of the target. In the next section we will extend the development of the $Q^2$ maneuver detector to encompass noisy measurements and estimates of the target state.

Fixing acceleration as output of the GDS model utilized to derive the $Q^2$ maneuver detector further constrains acceleration to be a state variable of the GDS model. The GDS output function becomes

$$a(t) = g\big(v(t), a(t)\big), \tag{7}$$

where $v(t)$ is velocity and $a(t)$ is acceleration. The state transition function then consists of the following set of equations

$$v(t + \Delta t) = v(t) + a(t)\Delta t, \qquad a(t + \Delta t) = \frac{2(x(t) + v(t)\Delta t)}{\Delta t^2}, \tag{8}$$

where $x(t)$ is position input and $\Delta t$ is the sample interval.

Using the GDS model of the target, the QDS model can be constructed. The qualitative output abstraction function, which maps the acceleration output of the GDS to the set $\{\omega_+, \omega_0, \omega_-\}$ is

$$\chi_W(a) = \begin{cases} \omega_+, & a \geqslant a_{\mathrm{m}}, \\ \omega_0, & a_{\mathrm{m}} \geqslant a \geqslant -a_{\mathrm{m}}, \\ \omega_-, & a \leqslant -a_{\mathrm{m}}. \end{cases} \tag{9}$$

The symbol $\omega_+$ corresponds to a maneuver whose acceleration is greater than $a_{\mathrm{m}}$, $\omega_0$ to a non-maneuver and $\omega_-$ to a maneuver whose acceleration is less than $-a_{\mathrm{m}}$. The construction of the qualitative state abstraction function $\chi_Q$ is parallel to the construction of $\chi_W$ since $a(t)$ is both the output and state variable:

$$\chi_Q(v, a) = \begin{cases} \theta_+, & a \geqslant a_{\mathrm{m}}, \\ \theta_0, & a_{\mathrm{m}} \geqslant a \geqslant a_{\mathrm{m}}, \\ \theta_-, & a \leqslant -a_{\mathrm{m}}. \end{cases} \tag{10}$$

The qualitative input event abstraction function, $\chi_P$, maps the input time set, inputs and previous states to three qualitative input events. The $Q^2$ hyperlimit partitions used by $\chi_P$ correspond to $a_{\mathrm{m}}$ and $-a_{\mathrm{m}}$ in the state space. These partitions are

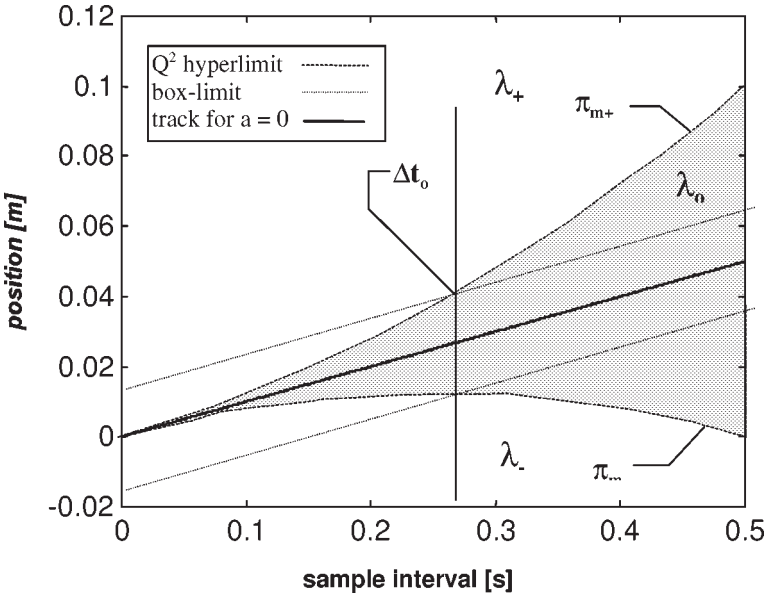


*Figure 2.* Projection of boxes and $Q^2$ hyperlimits used for maneuver detection from the input space $X \times V \times T$ to the $X \times T$ space for $v_m(t) = 0.1$. The region above $\pi_{m+}$ is the partition $\lambda_+$, the shaded region is $\lambda_0$ and the region below $\pi_{m-}$ is $\lambda_-$.

obtained by fixing acceleration in the second state equation and obtaining the following two hyperlimits:

$$\begin{aligned} \pi_{m+} &= \left\{ (\Delta t, x, v, a_m): \frac{2(x + v\Delta t)}{\Delta t^2} = a_m \right\}, \\ \pi_{m-} &= \left\{ (\Delta t, x, v, a_m): \frac{2(x + v\Delta t)}{\Delta t^2} = -a_m \right\}. \end{aligned} \tag{11}$$

The hyperlimits $\pi_{m+}$ and $\pi_{m-}$ delimit three qualitative input events $\{\lambda_+, \lambda_0, \lambda_-\}$, where $\chi_P$ maps all inputs into one of these regions

$$\chi_P(\Delta t, x, v) = \begin{cases} \lambda_+, & x \geqslant v\Delta t + \frac{1}{2}a_m\Delta t^2, \\ \lambda_0, & v\Delta t + \frac{1}{2}a_m\Delta t^2 > x > v\Delta t - \frac{1}{2}a_m\Delta t^2, \\ \lambda_-, & x \leqslant v\Delta t - \frac{1}{2}a_m\Delta t^2. \end{cases} \tag{12}$$

Alternatively, with the boxes approach we map the distinguishing point $a_m$ to the comparable distinguishing point $\Delta x_b$ in the output space. A maneuver is detected when the $x$ is contained in the following set

$$\chi_{Box}(\Delta t, x, v) = \begin{cases} \lambda_{Box+}, & x \geqslant v\Delta t + \Delta x_b, \\ \lambda_{Box0}, & v\Delta t + \Delta x_b > x > v\Delta t - \Delta x_b, \\ \lambda_{Box-}, & x \leqslant v\Delta t - \Delta x_b. \end{cases} \tag{13}$$

Figure 2 shows the difference between the $\chi_P$ and $\chi_{Box}$ partitions for a $X \times T$ projection of the input space $X \times V \times T$. The horizontal axis is the sample interval

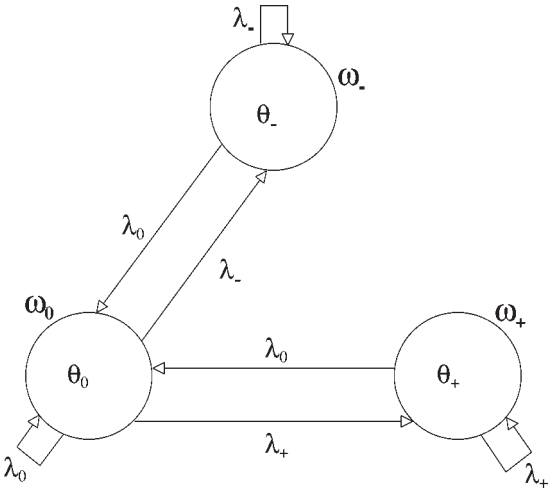


*Figure 3.* A Moore machine representation of the QDS for maneuver detection.

and the vertical axis is the position relative to the start of the sample interval. The figure shows that for time interval $\Delta t_0$ the $Q^2$ hyperlimit and the box-limit coincide. If our plant was limited to sample intervals of this duration, the performance of a hyperlimit and box-limit would be the same.

Concluding our formulation of maneuver detection with the $Q^2$ methodology we construct the Deterministic Finite Automaton (DFA) that completes the QDS. The DFA has three states from the set $\{\theta_+, \theta_0, \theta_-\}$, three inputs from the set $\{\lambda_+, \lambda_0, \lambda_-\}$ and three outputs from the set $\{\omega_+, \omega_0, \omega_-\}$. Figure 2 shows the three regions corresponding to $\{\lambda_+, \lambda_0, \lambda_-\}$ while Figure 3 shows the relationship between these three sets using a Moore Machine model, a DFA where output is associated with state.

### 3.4. $Q^2$ MANEUVER DETECTION

In this section the $Q^2$ maneuver detector is extended to encompass noisy measurements and estimates of the target state. When measurements are noisy the tracking community estimates state with a Kalman filter; the measurement residuals resulting from the estimation are then utilized to detect maneuvers. We show that the measurement residual can be substituted into the $\chi_P$ developed in the previous section and in the process extend $\chi_P$ and $Q^2$ to noisy measurements.

The position measurement residual is defined as the difference between the position measurement and the predicted position, $v = x - \hat{x}$. Since the Kalman filter utilizes the constant velocity model

$$x(t + \Delta t) = x(t) + v(t)\Delta t \tag{14}$$

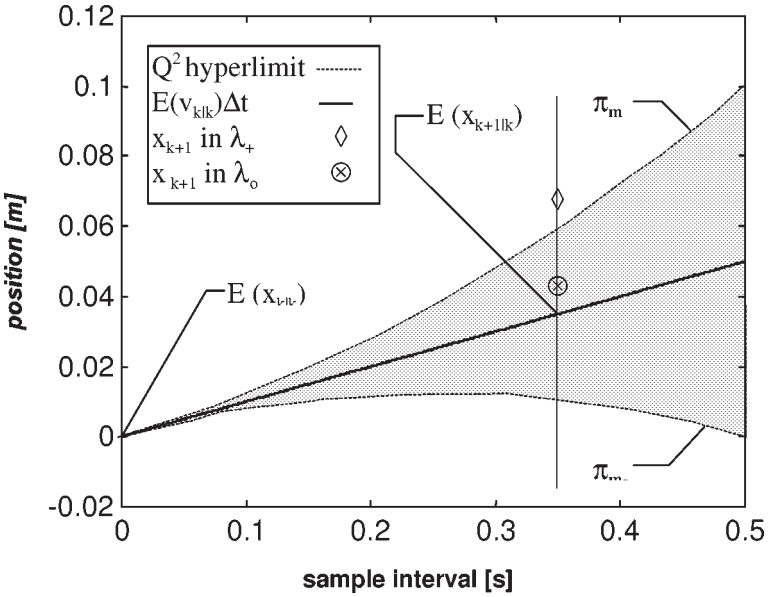


*Figure 4.* Projection of $Q^2$ hyperlimits from the input space $X \times V \times T$ to the $X \times T$ space with the origin set to $E(x_{k|k})$ and $E(v_{k|k}) = 0.1$.

the residual becomes $\nu = x - \tilde{v}\Delta t$. In order to represent maneuver detection in terms that are familiar to the tracking community, the inequalities (12) can now be manipulated to include the residual term:

$$\chi_P(\Delta t, x, v) = \begin{cases} \lambda_+, & \nu = x - \tilde{v}\Delta t \geqslant \frac{1}{2}a_{\mathrm{m}}\Delta t^2, \\ \lambda_0, & \frac{1}{2}\tilde{a}\Delta t^2 > \nu = x - \tilde{v}\Delta t > -\frac{1}{2}a_{\mathrm{m}}\Delta t^2, \\ \lambda_-, & \nu = x - \tilde{v}\Delta t \leqslant -\frac{1}{2}a_{\mathrm{m}}\Delta t^2. \end{cases} \tag{15}$$

With the inclusion of $\nu$ into our analysis, $\chi_P$ partitions position based on a prediction of position and a noisy measurement; the partition is performed without knowing the true position of the target, effectively setting the origin of the graph in Figure 2 to $E(x_{k|k})$ and using the estimate of velocity, $E(v_{k|k})$ to set the slope of the straight line ($a = 0$). While the new graph shown in Figure 4 has the same form as the graph in Figure 2, the new graph partitions estimates of state rather than actual state of the target.

The relationship between the plant, position measurements, the Kalman filtering, the quantitative GDS model and the qualitative QDS plant model, used by the $Q^2$ based maneuver detector is shown in Figure 5. We begin maneuver detection by taking position measurement from the plant and then calculating an estimate of the target state using a Kalman filter with a constant velocity model. The qualitative input abstraction function takes the position measurement $x$, the velocity estimate $\tilde{v}$ and the sample interval $\Delta t$ and derives the qualitative input to the automaton.

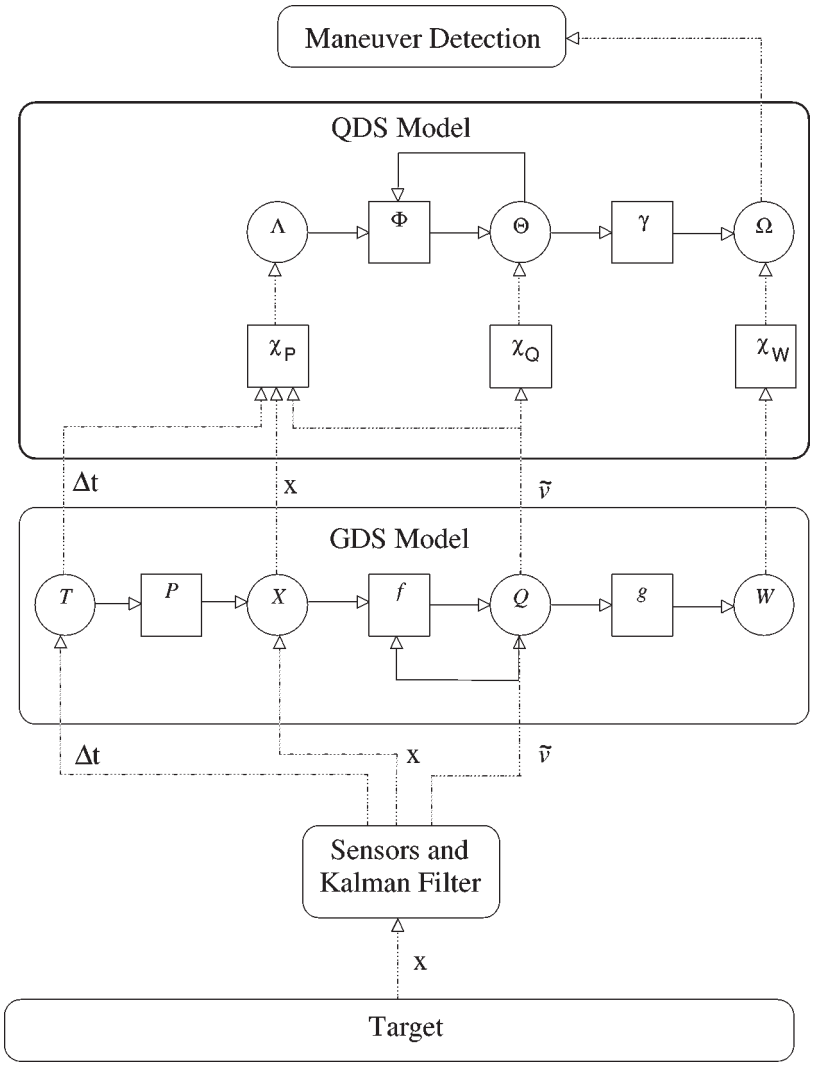


*Figure 5.* Relationship between target, measurements, Kalman filtering, the quantitative GDS model and the qualitative QDS model of the plant.

The automaton's next state gives an output that is a qualitative abstraction of the plant's acceleration: maneuver or non-maneuver.

## 4. Experimental Description

Our experiments compare the efficacy of the $Q^2$ maneuver detector versus the hyperbox maneuver detector. We ran numerous trials at different levels of detector sensitivity for the generation of Receiver Operation Characteristic (ROC) curves.

The ROC curves allow a performance comparison of the two detectors for different noise levels.

The following sections describe our experiment trials, the definition of the maneuver $a_{\mathrm{m}}$, detector sensitivity, generation of ROC curves and our simulation results. Our experiment was coded using Matlab$^{\mathrm{TM}}$ version 4.2c.

### 4.1. EXPERIMENTAL TRIAL DESCRIPTION

We simulate the discrete target described in Equations (5) and (6) with a time step $T = 5$ msec. The deterministic target input $u(t)$ is a single fixed maneuver consisting of an acceleration step of amplitude $a_p = 0.1$ m/sec.$^2$ that occurs 0.1 sec. after the start of the simulation. We estimate target state with a Kalman filter using the constant-velocity model shown in Equation (14).

In order to settle the Kalman filter in a controlled manner the target is tracked before the maneuver with a sample interval of 5 msec. Then our maneuver detector performs one single detection at a sample interval $\Delta t$ after the onset of the acceleration step (at 0.1 sec.). Individual trials are performed using one of the eight sample interval durations in the range of 40 to 80 msec. Different sampling intervals are used in different trials since both detectors are equivalent when utilizing only a single sample interval. This variation allows effective comparison of the efficacy of the partitions used by the two maneuver detectors.

### 4.2. MANEUVER DEFINITION

Our experiment is constructed so that half the trials use a maneuver definition $a_{\mathrm{m1}}$ that without noise would always result in a classification of maneuver by the detector. The other half of the experiments however use a higher maneuver threshold $a_{\mathrm{m2}}$, greater than the deterministic step input $a_p$, which would in a noise-free trial always result in a classification of non-maneuver. Our experiment was limited to positive accelerations so we did not utilize the $-a_{\mathrm{m}}$ threshold described in Section 3.3. The detectors are tested with both positive and negative examples of maneuvers so that we can measure both the detectors' probability of detection and their probability of generating false alarms. We selected two distinguishing points, $a_{\mathrm{m1}}$ and $a_{\mathrm{m2}}$, equidistant from $a_p$

$$a_{\mathrm{m1}} = a_p - \Delta a_{\mathrm{m}}, \qquad a_{\mathrm{m2}} = a_p + \Delta a_{\mathrm{m}} \tag{16}$$

(with $\Delta a_{\mathrm{m}} = 0.0007$ m/sec.$^2$) so that the detection of maneuvers and non-maneuvers is equally difficult. Figure 6 shows the $X \times T$ projection from the input space $X \times V \times T$ of the $\mathrm{Q}^2$ hyperlimits $\pi_{\mathrm{m1}}$ and $\pi_{\mathrm{m2}}$ for the two distinguishing points $a_{\mathrm{m1}}$ and $a_{\mathrm{m2}}$, respectively. Also included in Figure 6 are the curves for the partitions $\pi_{\mathrm{min}}$ and $\pi_{\mathrm{max}}$; these partitions are related to the generation of ROC curves and are explained in the following section.

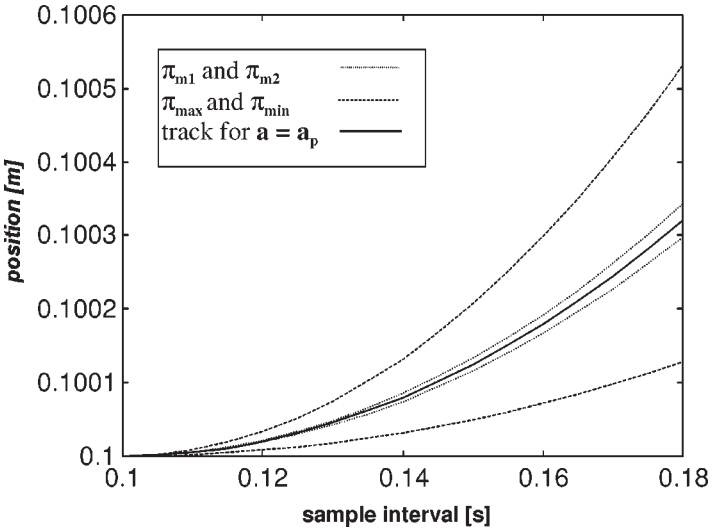


*Figure 6.* The $X \times T$ projection from the input space $X \times V \times T$ of the $Q^2$ hyperlimits $\pi_{m1}$ and $\pi_{m2}$ and the $Q^2$ hyperlimits for the largest and smallest tolerance levels, $\pi_{min}$ and $\pi_{max}$, respectively.

### 4.3. DETECTOR SENSITIVITY AND ROC CURVES

Our experiment is constructed to show the relative performance of the $Q^2$ and hyperbox maneuver detectors over a range of detector sensitivity. By varying the sensitivity of the detector we can vary proportionally the detector's Probability of False Alarm (PFA). The superior detector will have a higher Probability of Detection (PD) for the entire range of PFA. This tradeoff between PFA and PD is often shown graphically in ROC curve.

We construct the ROC curve by adjusting the independent variable, PFA. Our experiment adjusts PFA by adding a sensitivity threshold $\Delta a_t$ to our distinguishing point. We do not change truth, our definition of maneuver $a_m$ but we do adjust the threshold at which we believe that our measurement actually is indicative of a maneuver.

A negative sensitivity threshold increases the sensitivity of the maneuver detector while a positive sensitivity threshold decreases the sensitivity. Figure 6 shows the $X \times T$ projection from the input space $X \times V \times T$ of the $Q^2$ hyperlimits $\pi_{max}$ and $\pi_{min}$ for the two distinguishing points $a_{m1} + \Delta a_t$ and $a_{m2} - \Delta a_t$, respectively. The upper hyperlimit $\pi_{max}$ generates the highest PFA and the lower limit $\pi_{min}$ generates the lowest PFA.

### 4.4. RESULTS

Performance for the $Q^2$ and box based maneuver detectors was compared for twenty different levels of measurement noise. At each noise level we generated a ROC

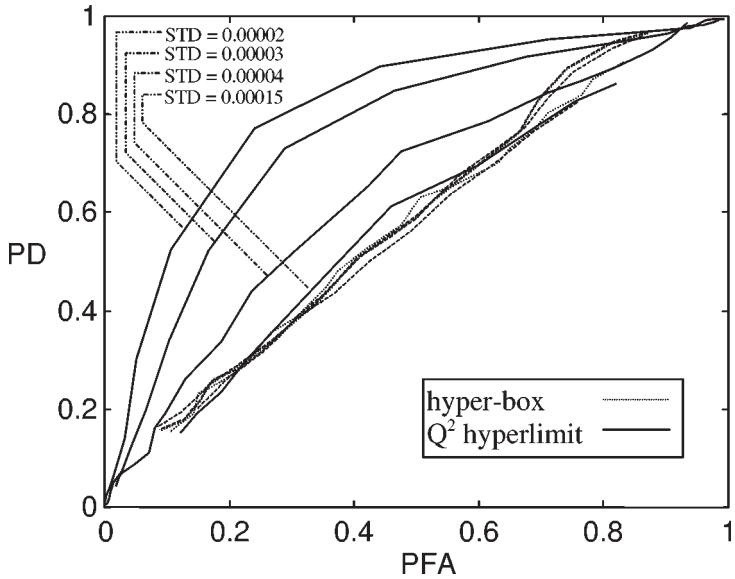


*Figure 7.* Probability of Detection (PD) versus Probability of False Alarm (PFA) for different measurement noise levels ($Q^2$ hyperlimit based detector – solid lines, box based detector – dashed lines).

curve from 21 points; each point for a different level of PFA. The different levels of PFA were generated by varying the tolerance level $\Delta a_t$ by a constant step of 0.005 m/sec.$^2$ Statistics for each tolerance level were accumulated for each of the eight sample intervals used, with 25 trials performed using each sample interval.

The superior performance of the $Q^2$ maneuver detector is shown with four representative ROC curves, for the noise levels with standard deviation of 0.00002, 0.00003, 0.00004 and 0.00015, in Figure 7. These curves show that as the noise level increases the performance of the $Q^2$ maneuver detector declines and at a noise level of 0.00015 the performance approaches the level of the box based maneuver detector. The performance of the box based maneuver detector shows no appreciable change with varying noise level.

The shape of the ROC curves generated is specific to the set of parameters we used for our experiment. Varying the tolerance levels over a different range and utilizing different maneuver definitions vary the shape of the ROC curves dramatically. In all cases tested we found that the $Q^2$ based maneuver detector outperformed the box based maneuver detector.

## 5. Discussion and Conclusion

The $Q^2$ methodology generates a minimal consistent qualitative partition of a GDS model of a plant. While logical consistency can be proven between the noise-free GDS model and the qualitative QDS model generated by $Q^2$, in the presence of

measurement noise logical consistency can not be proven between the plant and the QDS model. The goal of this research is to demonstrate that the $Q^2$ partition is robust in the presence of noise even though the $Q^2$ partition is not provably consistent. We selected the domain of maneuver detection to show that the minimal $Q^2$ partition is superior to the standard box partition. Our experiments show that for reasonable levels of noise, the hypersurface partitions generated by the $Q^2$ methodology are superior to hyperboxes in detecting maneuvers, and at high level of noise the $Q^2$ produces results that are no worse than the hyperbox methodology.

When designing our simulation scenario we made certain assumptions that may not hold in more complex domains: that the GDS model of the plant is available, and that the plant is time invariant. Several unanswered questions need to be resolved by future research. Given that an a priori GDS model is not available for a plant is it necessary to construct a GDS model from observations before constructing the QDS model, or can the QDS be constructed directly, without knowing the structure of the GDS model?

The results of this research are applicable to real world maneuver detection. Through our experiments, we have shown that the application of the $Q^2$ methodology can improve the performance of the maneuver detector over the standard box based detector.

Our simple maneuver detection simulation is easily enhanced to support more complex kinematic models. With a correspondingly more complex definition of maneuver we can show the full efficacy of a $Q^2$ based maneuver detector. The more complex scenario generates an automaton that contains more than the three states shown in Figure 3 for this paper's detector. With more states, meaningful symbolic reasoning can be performed on the possible input sequences needed to reach a goal state. Another enhancement to the detector, which would result in improved ROC curves for the detector, requires the utilization of more than one measurement to make a classification of maneuver or non-maneuver. Many real-world maneuver detectors use several measurements and a sliding likelihood filter. Our study can be expanded to show the effect of the $Q^2$ technique on the sliding likelihood filter algorithm.

## References

1. Albus, J. S.: Outline for a theory of intelligence, *IEEE Trans. Systems Man Cybernet.* **21** (1991), 473–509.
2. Alur, R., Courcoubetis, C., Heniznger, T. A., and Ho, P.-H.: Hybrid automata: An algorithmic approach to the specification and verification of hybrid systems, in: R. L. Grossman, A. Nerode, A. P. Ravn, and H. Rischel (eds), *Theory of Hybrid Systems*, Lecture Notes in Comput. Sci. 736, Springer, Berlin, 1993, pp. 209–229.
3. Antsaklis, P. J. et al.: Towards intelligent autonomous control systems: Architecture and fundamental issues, *Intelligent and Robotic Systems* **1** (1989), 315–342.
4. Bar-Shalom, Y. and Fortmann, T. E.: *Tracking and Data Association*, Academic Press, New York, 1988.
5. Blackman, S. S.: *Multiple-Target Tracking with Radar Applications*, Artech House, 1986.

6. Bolger, P. L.: Targeting a maneuvering target using input estimation, *IEEE Trans. Aerospace Electronic Systems* **23**(3) (1987), 298–310.
7. Branicky, M. S., Borkar, V. S., and Mitter, S. K.: A unified framework for hybrid control: Model and optimal control theory, *IEEE Trans. Automat. Control* **43**(1) (1998), 31–45.
8. Genesereth, M. R. and Nilsson, N. J.: *Logical Foundations of Artificial Intelligence*, Morgan Kaufman, Los Altos, CA, 1987.
9. Guckenheimer, J. and Johnson, S.: Planar hybrid systems, in: P. Antsaklis, W. Kohn, A. Nerode, and S. Sastry (eds), *Hybrid Systems II*, Lecture Notes in Comput. Sci. 999, Springer, Berlin, 1994.
10. Kokar, M. M.: Critical hypersurfaces and the quality space, in: *6th National Conf. on Artificial Intelligence*, AAAI, 1987.
11. Kokar, M. M.: Qualitative dynamics and fusion, in: *1st IEEE Conf. on Control Applications*, Dayton, OH, 1992.
12. Kokar, M. M.: On consistent symbolic representations of general dynamic systems, *IEEE Trans. Systems Man Cybernet.* **25**(8) (1995), 1231–1242.
13. Korona, Z. and Kokar, M. M.: A fusion and learning algorithm for landing aircraft tracking: Compensating for exhaust plume disturbance, *IEEE Trans. Aerospace Electronic Systems* **31**(3) (1995), 1210–1215.
14. Kuipers, B. J.: Qualitative simulation, *Artificial Intelligence J.* **29** (1986), 289–338.
15. Kuipers, B.: *Qualitative Reasoning: Modeling and Simulation with Incomplete Knowledge*, MIT Press, Cambridge, MA, 1994.
16. Lemmon, M., Stiver, J. A. et al.: Event identification and intelligent hybrid control, in: A. Nerode and W. Kohn (eds), *Hybrid Systems*, Lecture Notes in Comput. Sci. 736, Springer, Berlin, 1993.
17. Mesarovic, M. D. and Takahara, Y.: *Abstract System Theory*, Springer, Berlin, 1989.
18. Nerode, A. and Kohn, W.: Models for hybrid systems: Automata, topologies, controllability, observability, in: A. Nerode and W. Kohn (eds), *Hybrid Systems*, Lecture Notes in Comput. Sci. 736, Springer, Berlin, 1993.
19. Puri, A. and Varaiya, P.: Verification of hybrid systems using abstractions, in: P. Antsaklis, W. Kohn, A. Nerode, and S. Shastry (eds), *Hybrid Systems II*, Lecture Notes in Comput. Sci. 735, Springer, Berlin, 1995, pp. 359–369.
20. Strauss, P.: Problems of interval-based qualitative reasoning, in: D. S. Weld and J. deKleer (eds), *Readings in Qualitative Reasoning about Physical Systems*, Morgan Kaufman, Los Altos, CA, 1990, pp. 288–305.